Brain Source Localization in the Presence of Leadfield Perturbations

Rabiya Momin, *Student Member*, IEEE, Hasan S. Mir, *Senior Member*, IEEE and
Hasan Al-Nashash, *Senior Member*, IEEE

***Abstract*— This paper studies the performance of the recently developed G-MUSIC algorithm as applied to the problem of brain source localization. G-MUSIC is a form of weighted MUSIC that performs better in scenarios where only limited sample support is available. Two transfer function based calibration algorithms are also developed to estimate the location of neural activity in the brain accurately when the measured leadfield is perturbed. The localization performance of G-MUSIC is compared to traditional MUSIC and quantified in terms of the localization error. Simulations suggest that G-MUSIC can offer significantly improved localization accuracy over conventional MUSIC. *Index Terms*—Brain source localization, inverse problem, G-MUSIC, calibration.**

I. Introduction

Brain source localization focuses on localizing different regions that are activated in the brain during a given mental task. Electroencephalography (EEG) is a noninvasive technique that measures electric potentials due to any neural activity in the brain Due to its low hardware costs and high temporal resolution, EEG provides an alternative neuroimaging technique to positron emission tomography (PET) and functional magnetic resonance imaging (fMRI). Moreover, EEG offers the possibility of measuring neuronal activity in real time, as needed when investigating the temporal properties of the brain [1]. In the context of EEG, the bio electromagnetic *inverse* problem consists of localizing the source of signals collected in response to neural activity.

Array processing methods provide a robust signal processing tool to solve the inverse problem. MUltiple SIgnal Classification (MUSIC) is a well-known subspace-based source localization algorithm that utilizes the eigen structure of the spatial covariance matrix and provides a computationally efficient alternative to maximum likelihood (ML) algorithms [2]. Improved localization accuracy is afforded through the use of more electrodes; this in turn requires more time samples in order to obtain an accurate estimate of the data covariance matrix. However, enough time samples may not be available or usable due to the nonstationarity property of the signal. Nonstationarity could arise due to different time scales involved in the dynamical process, which for EEG waves is on the order of 0.1 seconds whereas that of an action potential is about 1millisecond [3].

R. Momin is a graduate student at the Department of Electrical Engineering, American University of Sharjah, UAE(g00037087@aus.edu)
H. Mir is with the Department of Electrical Engineering, American University of Sharjah, UAE (e-mail:hmir@aus.edu).
H. Al-Nashash is with the Department of Electrical Engineering, American University of Sharjah, UAE (e-mail: hnashash@aus.edu).

In cases where only a limited number of samples are available, the performance of the MUSIC algorithm degrades since part of the energy from the noise subspace of the covariance matrix leaks into the signal subspace, causing the two subspaces to lose their orthogonality. In order to counter this problem, a new source localization technique called G-MUSIC is proposed in [4] which is a form of weighted MUSIC. Unlike MUSIC which only uses eigenvectors from the noise subspace, G-MUSIC uses all (signal and noise) eigenvectors of the data covariance matrix.

Furthermore, various anomalies can cause the measured lead field to differ from the theoretical lead field. These anomalies can arise due to e.g. co-registration and approximation of the head model with limited accuracy and discretization of the source space and are termed as calibration errors [5]. As such, array calibration is required to account for any discrepancies that may cause the actual lead-field to differ from the theoretical one [6]. This paper develops a combined calibration and localization framework for EEG systems operating in the limited sample regime. The performance of the calibration technique coupled with G- MUSIC is assessed and compared against the traditional MUSIC algorithm in terms of the source localization error.

The rest of the paper is organized as follows. Section II reviews the G-MUSIC algorithm. Section III introduces the external and autocalibration algorithms. The simulation setup and quantification of results is presented in section IV, followed by the conclusion in section V.

II. Methodology

A. Signal Model

Consider the collection of K signals for N time samples obtained from an array of M sensors

$$\boldsymbol{y}(\boldsymbol{n}) = \boldsymbol{V}\boldsymbol{x}(n) + \boldsymbol{w}(n) \tag{1}$$

$\boldsymbol{V}$ is an M x K normalized lead field matrix that is obtained from the forward problem solution, $\boldsymbol{x}\ (n)$ is a K x 1 source vector and $\boldsymbol{w}\ (n)$ is zero mean additive Gaussian noise at time n. Then, the true M x M covariance matrix of the observation can be represented as

$$\boldsymbol{R} = \boldsymbol{V}\, R_{xx}\, \boldsymbol{V}^{H} + \sigma^2\, \boldsymbol{I}_M \tag{2}$$

where, $\sigma^2\ I_{\mathrm{M}}$ and R_{xx} denote the noise and the source correlation matrix, respectively. Furthermore, we denote the eigenvectors of $\boldsymbol{R}$ as $\{e_i,\ i= 1.....M\}$ and its eigenvalues as

$\omega_1 \leq \omega_2 \leq \cdots . \omega_M$. Assuming $M \geq K$, the smallest M - K eigenvalues of $\boldsymbol{R}$ correspond to the noise subspace. The eigen decomposition of $\boldsymbol{R}$ is represented as

$$\boldsymbol{R} = \boldsymbol{E_S \Lambda_S E_S^H} + \sigma^2 \boldsymbol{E_N}\, \boldsymbol{E_N^H} \tag{3}$$

where, $\boldsymbol{E_S} = [\boldsymbol{e_1} .. \boldsymbol{e_K}] \in \mathrm{R}^{M\,X\,K}$ $\boldsymbol{E_N} = [\boldsymbol{e_{K+1}} .. \boldsymbol{e_M}] \in R^{M\,X\,M-K}$ denote the signal and noise subspace and $\boldsymbol{\Lambda}_S$ represents the diagonal matrix containing the eigenvalues that correspond to the signal subspace.The basic idea behind subspace identification algorithms such as MUSIC is based on the property that any vector present in the signal subspace is orthogonal to the noise subspace, i.e. $\boldsymbol{E_N}^T \boldsymbol{v_k} = 0$.

In reality, however the eigenvectors are not known a-priori and must be estimated from the received signal. We denote the sample covariance matrix as $\widehat{\boldsymbol{R}}_N = \frac{1}{N} \sum_{\boldsymbol{n}} \mathbf{y}(n)\mathbf{y}(n)^{\boldsymbol{T}}$ and its assosciated eigenvectors as $\{\hat{e}_i,\ i = 1 \ldots .M\}$ and eigenvalues as $\lambda_1 \leq \lambda_2 \leq \cdots \lambda_M$.

The noise eigenvectors $\widehat{\boldsymbol{E}}_N$of the sample covariance matrix are not exactly equal to $\boldsymbol{E}_N$; therefore $\widehat{\boldsymbol{E}}_N{}^H \boldsymbol{v_k}$ should have a small (but non-zero) norm. The MUSIC algorithm exploits this principle by searching for the deepest local minima of the cost function

$$\eta_{MUSIC=}\ \boldsymbol{v_k^T}\, \widehat{\boldsymbol{E}}_N\, \widehat{\boldsymbol{E}}_N{}^T \boldsymbol{v}_k \tag{4}$$

Keeping the number of sensors (M) fixed and making appropriate statistical assumptions where the number of samples (N) increases without bound ($N \rightarrow \infty$), the MUSIC cost function is a good estimate of the deterministic original cost function. MUSIC is thus considered to be N- consistent; however the algorithm breaks down when the number of samples fall below a certain threshold, as shown in [4].

B. Mathematical Formulation of G-MUSIC [4]

In order to localize sources when only finite sample support is available a new weighted MUSIC estimator is proposed that is both *M, N* consistent.

The tools used to improve the asymptotic performance of MUSIC are based on G-estimation techniques that exploit results from random matrix theory. This method helps derive an *M, N* consistent estimator of the true covariance matrix for different scalar functions. Such an estimator is referred to as G-MUSIC. The cost function is defined as

$$\eta_{\text{G-MUSIC}=}\ \boldsymbol{v}_k^T \left(\sum_{i=1}^{M} \varphi(i) \hat{e}_i \hat{e}_i^T \right) \boldsymbol{v}_k \tag{5}$$

where,

$$\varphi(\mathrm{i}) = \begin{cases} 1 + \sum_{\mathrm{k=M-K+1}}^{\mathrm{M}} \frac{\lambda_k}{\lambda_i - \lambda_k} - \frac{\mu_k}{\lambda_i - \mu_k} & \mathrm{i} \leq \mathrm{M\text{-}K} \\ -\sum_{\mathrm{k=1}}^{\mathrm{M-k}} \frac{\lambda_k}{\lambda_i - \lambda_k} - \frac{\mu_k}{\lambda_i - \mu_k} & \mathrm{i} > \mathrm{M\text{-}K} \end{cases} \tag{6}$$

and $\mu_1 \leq \mu_2 \leq \cdots \ldots \leq \mu_M$ are the eigenvalues of *diag* $(\boldsymbol{\lambda})$ $-\frac{1}{N} \sqrt{\boldsymbol{\lambda}}\, \sqrt{\boldsymbol{\lambda}}^T$.

It can be seen from (6) that G-MUSIC uses all the eigenvectors of the covariance matrix, whereas MUSIC only uses the eigenvectors corresponding to the noise subspace. The signal subspace is included in the G-MUSIC estimator since low sample support causes the noise subspace to leak into the signal subspace which in turn makes the two slightly non- orthogonal.

III. CALIBRATION

In order to relate the modeled and measured leadfield, transfer function based calibration algorithms are now developed. These algorithms require prior knowledge about the geometry of the modeled array manifold and the leadfield of the guide sources. Guide sources can be obtained by collecting strong focal evoked responses in the functionally mapped parts of the brain using applicable stimulation (auditory, somatosensory, visual, etc.). These accumulated evoked responses correspond to the measured/actual leadfield of the guide sources [5].

1) External Calibration

Assuming that the locations of L guide sources *(*$L \geq M$*)* are known, the modeled and measured leadfield are defined as follows:

$$\boldsymbol{V} \triangleq [v_1 \ldots . . v_L] \tag{7}$$

$$\boldsymbol{Z} \triangleq [z_1 \ldots . . z_L] \tag{8}$$

The calibration matrix $\boldsymbol{A} \in \mathrm{R}^{M\mathrm{x}M}$ is then computed such that, $\boldsymbol{Z} \approx \boldsymbol{AV}$, i.e. the modeled leadfield is a good approximation of the measured leadfield.

Two cost functions are defined in order to quantify the goodness of the approximation:

Least Squares Criterion[5]: Define the cost function as*:*

$$\boldsymbol{J}_{LS} \triangleq \sum_{l=1}^{L} ||\boldsymbol{z}_l - \boldsymbol{A}\boldsymbol{v}_l||_F^2 \tag{9}$$

Where, F denotes the Frobenius norm. Minimizing the above cost function yields:

$$\boldsymbol{A} = \boldsymbol{Z}\, \boldsymbol{V}^T (\boldsymbol{V}\boldsymbol{V}^T)^{-1} = \boldsymbol{Z}\boldsymbol{V}^{\#} \tag{10}$$

Beamsum Criterion: An alternative cost-function to least-squares is also presented in this paper. Consider introducing an additional degree of freedom in (9) as:

$$\boldsymbol{J}_{BS} \triangleq \sum_{l=1}^{L} ||\boldsymbol{z}_l - \alpha_l \boldsymbol{A}\boldsymbol{v}_l||_F^2 \tag{11}$$

The optimum solution for $\alpha_l$is given by

$$\alpha_l = \frac{(\boldsymbol{AV})^H \boldsymbol{Z}}{||\boldsymbol{AV}||^2} \tag{12}$$

α_l can be viewed as the projection of the modeled leadfield onto the measured leadfield. The primary disadvantage of external calibration is that any changes in the environment will not be accounted for and will require the calibration to be repeated.

2) Auto Calibration:

Contrary to external calibration, auto calibration only requires approximate information about the locations of the guide sources. This technique employs a sequential optimization procedure to refine the estimates of the source

locations and then update the calibration parameters according to changes in the environment. An initial estimate of the source locations is obtained provided that nominal knowledge of the calibration matrix is available.

We define $\bar{V}$ as the modeled leadfield of *estimated* source locations and construct the calibration matrix. For least squares the calibration matrix is computed as

$$\bar{A} = Z\bar{V}^{\#} \tag{13}$$

The calibration matrix for beamsum is constructed by alternating between computing α_k from (12) and $\bar{A}$ as follows:

$$\bar{A} = \boldsymbol{Z}\left(\bar{V}\ \mathrm{diag}\left[\bar{\alpha}_1 \ldots \bar{\alpha}_l\right]\right)^{\#} \tag{14}$$

The initial guess for $\bar{A}$ is provided by (13). As long as the error associated with the initial guess is relatively small, the iterative algorithms will converge to its true solutions.

Fig.1 summarizes the iterative steps of the autocalibration algorithm.

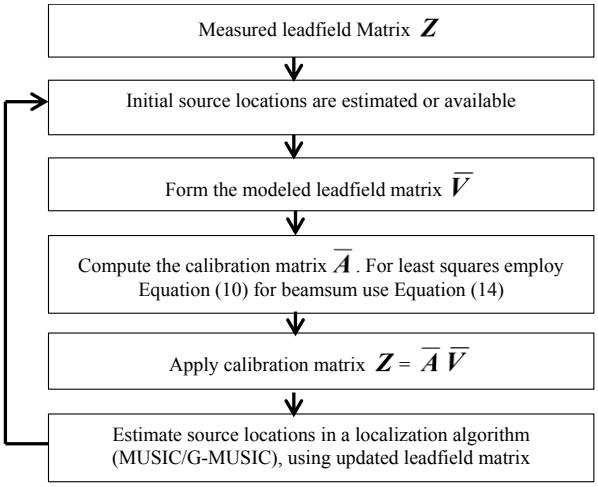

Fig.1: Flow diagram of the autocalibration process

IV. Simulation Results

The forward problem solution in this paper was obtained using the Brainstorm software. A three- shell spherical head model is used and the head model computations have been done on the Colin27 head anatomy with resolution 1mm, which is an MRI volume provided by the Montreal Neurological Institute [8]. Next, synthetic EEG signals were produced for a BioSemi 64 electrode system (*M=64*). The modeled leadfield is obtained from Brainstorm and the perturbed measured leadfield is modeled as in [5]:

$$\boldsymbol{Z} = (\boldsymbol{A} + \Delta\boldsymbol{A})\boldsymbol{V} \tag{15}$$

where $\boldsymbol{A}$ and $\Delta\boldsymbol{A}$ are *M x M* matrices, the elements of which correspond to zero mean normal distributions.

Initially, one of the four calibration techniques is used to account for any differences between the measured and modeled lead field matrices. For calibration, 65 guide sources (calibration points) were selected from 3840 possible source locations ($1/12^{th}$ of the entire cortex surface). Then, in order to verify the localization of 2 simulated random sources located at guide sources numbered 1710 and 2510 respectively (within the calibration region), the calibrated leadfield matrix is applied to either MUSIC or the G-MUSIC algorithm.

The effect of various calibration algorithms on the localization of sources was verified using G-MUSIC and MUSIC. Fig. 2 compares the mean squared error obtained by averaging over 30 realizations of the external and auto least squares calibration techniques for MUSIC and G-MUSIC.It can be seen that external least squares calibration applied to G-MUSIC has lower MSE compared to the other techniques as the number of samples decreases.

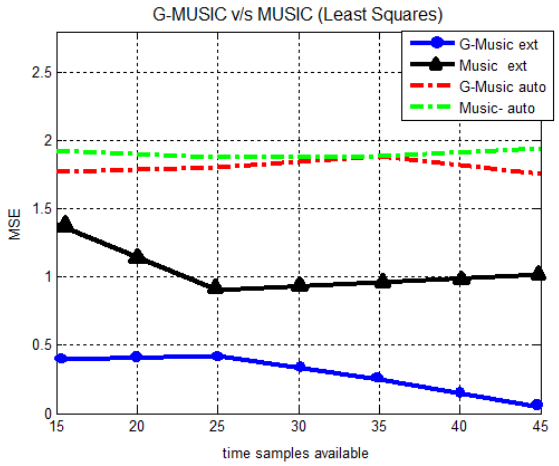

Fig.2: Comparative evaluation of the MSE achieved by MUSIC and G-MUSIC when least squares external and auto calibration techniques are applied.

The same results are observed for beamsum calibration and since, beamsum and least squares calibration produce comparable results the plots for beamsum are not included.

Fig.3 represents the localization error where a threshold was applied in order to identify the strongest peaks as the recovered sources. The locations of the recovered test sources were compared to the ideal locations (in this case 1710 and 2510), whichever it happened to be closer to. The simulations were carried out for 30 time samples with increasing SNR. In order to avoid repetition, localization error for only one of the sources is presented. Observe, that when external calibration is used, G-MUSIC has a lower localization error (measured in cm) than MUSIC.

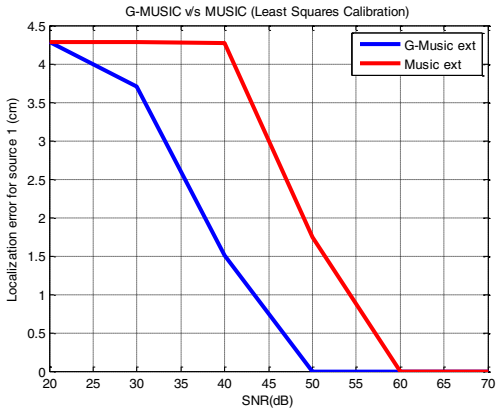

Fig.3: Least squares external calibration- comparative evaluation of the localization error achieved by MUSIC and G-MUSIC for source 1.

Similarly, Fig.4 suggests that G-MUSIC localizes sources with greater accuracy than MUSIC when least squares autocalibration is applied, even when small perturbations are introduced. Since, comparison of beamsum calibrations produce identical results, the plots are not included.

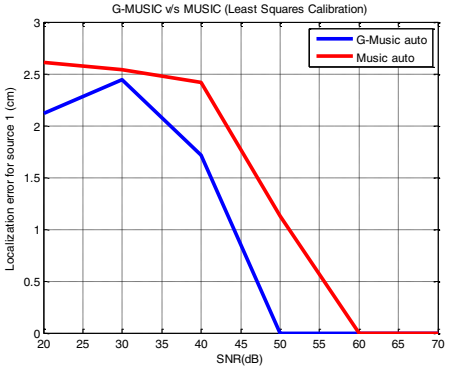

Fig.4: Least squares autocalibration-comparative evaluation of the localization error achieved by MUSIC and G-MUSIC for source 1.

Fig.5 shows that external least squares calibration provides lower localization error, in the presence of large leadfield perturbation when compared to the auto calibration least squares method, especially at higher SNR.

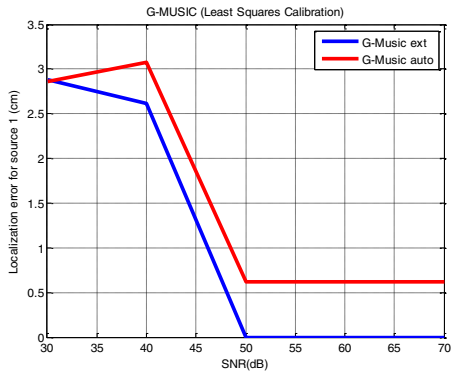

Fig.5: Comparative evaluation of the localization error achieved by least squares external and auto calibration for source 1.

Fig. 6 compares least squares autocalibration to beamsum autocalibration. It can be seen that the localization error for beamsum is lower than that of least squares at lower SNR.

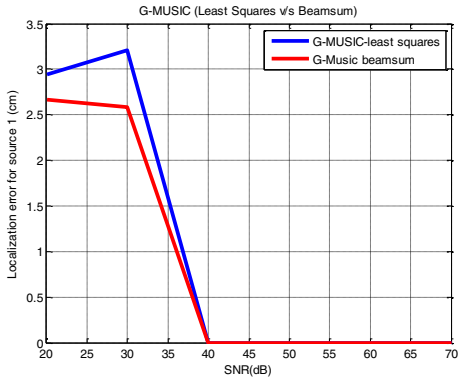

Fig.6: Auto calibration- comparative evaluation of the localization error achieved by least squares and beamsum autocalibration for source 1.

In all cases G-MUSIC outperforms MUSIC. Additionally, even though, in all cases external calibration outperforms autocalibration, it should be noted that external calibration assumes precise apriori knowledge of the guide source locations, whereas autocalibration only requires a nominal location estimate. Thus, autocalibration provides a more practical solution while still maintaining a localization performance similar to that achieved with external calibration.

V. Conclusion

In this paper, the performance of G-MUSIC and MUSIC was compared in the presence of leadfield perturbations when limited EEG sample size is available. Transfer function based external and auto calibration algorithms were applied in order to account for the perturbations. The least squares calibration algorithm minimizes the distance between the modeled and measured leadfields, and the beamsum calibration algorithm adds an additional degree of freedom by projecting the modeled leadfield onto the measured leadfield. Results suggest that G-MUSIC yields lower MSE and localization error than least squares external and auto calibration techniques applied to MUSIC even when the applied perturbation is very small. Moreover, G-MUSIC coupled with external least squares is superior to its autocalibration counterpart. The same pattern is observed when comparing external and auto beamsum calibration. Results also illustrate that G-MUSIC with beamsum autocalibration provides lower localization error than least squares autocalibration in low SNR environments.

References

[1] C. M. Michel, M. M. Murray, G. Lantz, S. Gonzalez, L. Spinelli, R. Peralta, "EEG source imaging," *Clinical Neurophysiology.*, vol. 115, no. 10, pp 2195-2222, Oct 2004.

[2] J.C. Mosher and R.M. Leahy, "Source localization using recursively appplied and projected (RAP) MUSIC," *IEEE Trans. Signal Processing*, vol. 47, pp. 332-340, 1999.

[3] P.P. Indic, R.R. Pratap, V.N. Nampoori, and N.N. Pradhan "Significance of Time Scales in Nonlinear Dynamical Analysis of EEG Signals," *Internation Journal of Neurosci.* , vol.99, no.1-4, pp. 181, Aug. 1999.

[4] X. Mestre, "An improved weighted MUSIC algorithm for small sample size scenarios," *in Proc. Adaptive Sensor Array Processing Workshop*, 2006.

[5] T. Zarghami, H.S. Mir, H.Nashash, "Calibration of Low Density EEG Sensor Arrays for Brain Source Localization," *Proceedings of 2013 International Conference on Neural Information Processing*, pp. 331 - 338, Nov. 2012

[6] H.S. Mir, J.D. Sahr, G.F. Hatke, and C.M. Keller, " Passive direction finding using an airborne sensor array in the presence of manifold perturbations," *IEEE Trans. Signal Process*., vol. 55,no.1,pp2486-2496,Jan.2007.

[7] J.J. Ermer, J.C. Mosher, S. Baillet , and R.M. Leahy, "Rapidly recomputable EEG forward models for realistic head shapes," *Phy.Med.Biol.,*vol. 46, no. 4, pp 1265-1281, Apr. 2001.

[8] S. Baillet, J.C. Mosher, and R.M. Leahy, "Electromagnetic brain mapping," *IEEE Signal Process. Mag*., vol. 18, no. 6, pp 14-30, Nov. 2001.

[9] F. Tadel, S. Baillet, J.C. Mosher, D. Pantazis, R.M. Leahy, "Brainstorm: A User-Friendly Application for MEG/EEG Analysis," *Comp. Intell. Neurosci*, 2011, pp.1-13, 2011.

[10] R. Couillet and M. Debbah, "Signal Processing in Large Systems: a New Paradigm," *IEEE Signal Process. Mag., vol.30*, no.1, pp. 24-39, 2013.